We sincerely thank the anonymous referee for their very helpful comments and for thoroughly reviewing the manuscript. The comments were very valuable and helpful in improving the clarity and quality of the manuscript. We have included all the comments and responded to them in detail below. Line numbers refer to the revised manuscript version.

Comment from anonymous reviewer (RC2)

Specific Comments:

1. I wonder if the extensive processing scheme is fully necessary, given reflections are quite strong in the raw data. For example, two rounds of curvelet filtering and spatial filtering via interpolation seem redundant. At the very least, could you provide more information about some of the key filtering parameters? Specifically, to remove ground roll?

➔ As you noted, the glacier-lake reflections in the raw radar data indeed exhibit high amplitude. Consequently, our data processing strategy prioritizes the preservation of these strong reflection signals while selectively attenuating various forms of noise—including random noise, crevasse-related noise, and ground roll—that may obscure meaningful subsurface features. The two rounds of curvelet-based filtering and spatial filtering via median interpolation (Anomalous Amplitude Attenuation (AAA) based on the Omega geophysical data processing platform from SLB) were carefully designed with distinct objectives at different stages of the workflow:

First Stage (Initial Filtering of Raw Data):
The initial AAA and curvelet filtering were applied to suppress high-frequency random noise and coherent linear noise that becomes prominent at later two-way travel times (beyond 2 seconds). These noise components are particularly detrimental to the identification of deep or weak reflectors, and their suppression enhances overall signal-to-noise ratio (SNR) without degrading the primary lake-related reflections.

Second Stage (Post-Processing Filtering):
Following surface-consistent deconvolution and gain corrections, residual noise structures—particularly remnants of ground roll and shallow-layer reverberations—persist in the dataset. The second round of curvelet filtering and AAA was implemented to target these residuals, improving the lateral continuity of true reflectors while further mitigating spatially coherent noise that could lead to misinterpretation.

To support transparency and reproducibility, we have included the processed field data and the parameters used at each major step in the revised Supplementary Materials. These examples demonstrate the efficacy of the adopted filtering scheme in retaining high-amplitude lake reflections while effectively eliminating noise.

2. In figures, be a bit more specific about geometry. Add a 21X' on one end for example to see which direction the record sections are. You can figure it out, but it might make them a bit clearer

➔ We have added a reference to Ju et al. (2025), which provides a detailed description of the subglacial lake boundaries inferred from ice-penetrating radar (IPR) surveys. The location of the seismic survey lines in this study was carefully determined based on the lake extent proposed by Ju et al. (2025). We updated Figure 3 to include the subglacial lake extent defined by Ju et al. (2025), along with a hydraulic head map, to provide more comprehensive spatial context for the survey design. Additionally, to help readers easily understand the orientation of the cross-sectional profiles in Figure 6, we added the X–X' line to Figure 3.

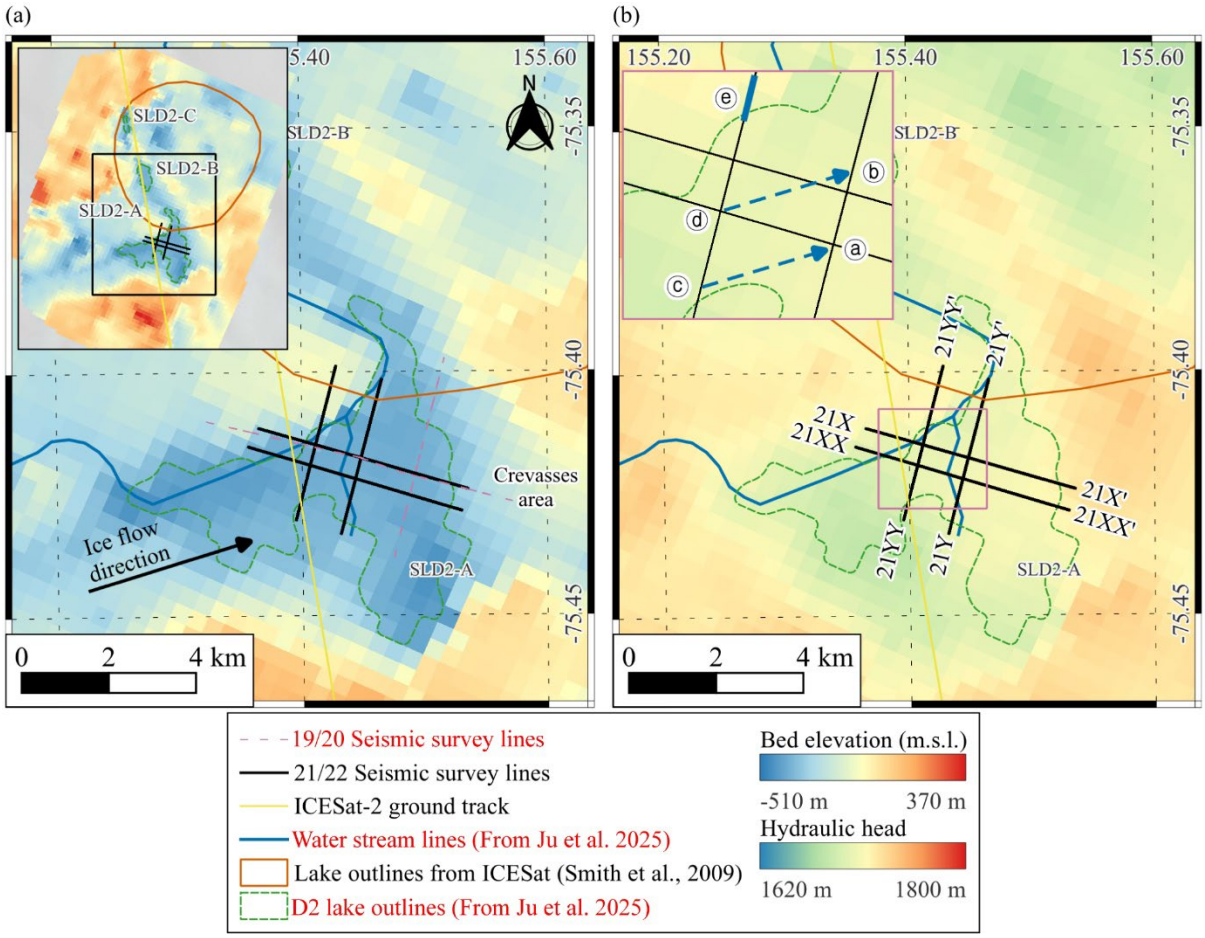

Figure 3: Seismic survey layout (black lines) overlaid on (a) bed elevation and (b) hydraulic head data from IPR results (Ju et al., 2025).

3. Figure 4 and 6: the colorbar is not appropriate. My understanding of what's plotted is the normalized seismic section between -1 and 1, which would be equal (or rather proportional, equal after accounting for geometric spreading, source, attenuation etc) to the reflection coefficient only at normal incidence. I think the colorbar should either be labelled as normalized stacked energy or actual units given.

➔ We have revised Figures 4 and 6 by changing the colorbar label from "Reflection coefficient" to "Normalized stacked energy" to represent the displayed seismic attributes more accurately.

4. On this point, I wonder why not try to calculate an absolute reflectivity curve (AVO Horgan et al. 2021; Peters et al. 2008) or relative reflectivity curve, to confirm you are truly seeing water at the base rather than some kind of wet sediment layer, which would also result in a negative polarity PP reflection. Even if you just do this for one of the lines, the coherence with the analytical reflectivity curve would make the argument much stronger.

➔ We sincerely appreciate the reviewer's valuable suggestion. We conducted seismic surveys in areas with a high likelihood of basal water presence, as indicated by radar observations, based on the recently published study by Ju et al. (2025). We fully acknowledge that AVO analysis is a powerful tool for distinguishing between basal water and wet sediments. However, AVO analysis typically requires a sufficiently wide range of incidence angles to derive reliable reflectivity curves. We think that conventional AVO analysis would be difficult to apply due to the limited offset range resulting from the short length of the seismic line.

We fully agree with the scientific merit of the approach suggested by the reviewer. In response, and as part of our ongoing efforts to enhance subsurface interpretation, we are planning further research aimed at implementing deghosting and AVO analysis, as well as developing a refined velocity model that incorporates detailed firn-layer velocity structures. These improvements are expected to facilitate more advanced seismic processing, higher-resolution imaging of subglacial lake structures, and ultimately a more accurate understanding of the basal environment in future investigations.

We have added content to the conclusion.
(Page 19, Line 370-373) "Furthermore, we plan to conduct follow-up studies incorporating advanced processing techniques such as deghosting, amplitude variation with offset (AVO) analysis, and the development of a refined velocity model that accounts for detailed firn-layer properties. These technical advancements are expected to enhance the resolution and precision of seismic imaging and contribute to a deeper understanding of the subglacial environment in future investigations."

5. Figure 6e: I'm a bit confused on the interpretation here. The glacier-bed ghost (4) appears to be normal polarity, while the direct reflection appears to be reverse polarity? This seems opposite to the discussion in the analysis. I'm wondering if I am seeing something wrong, or perhaps the color scale is flipped for this inset?

➔ We have enlarged Figure 6 to enhance clarity and make key features more visible.

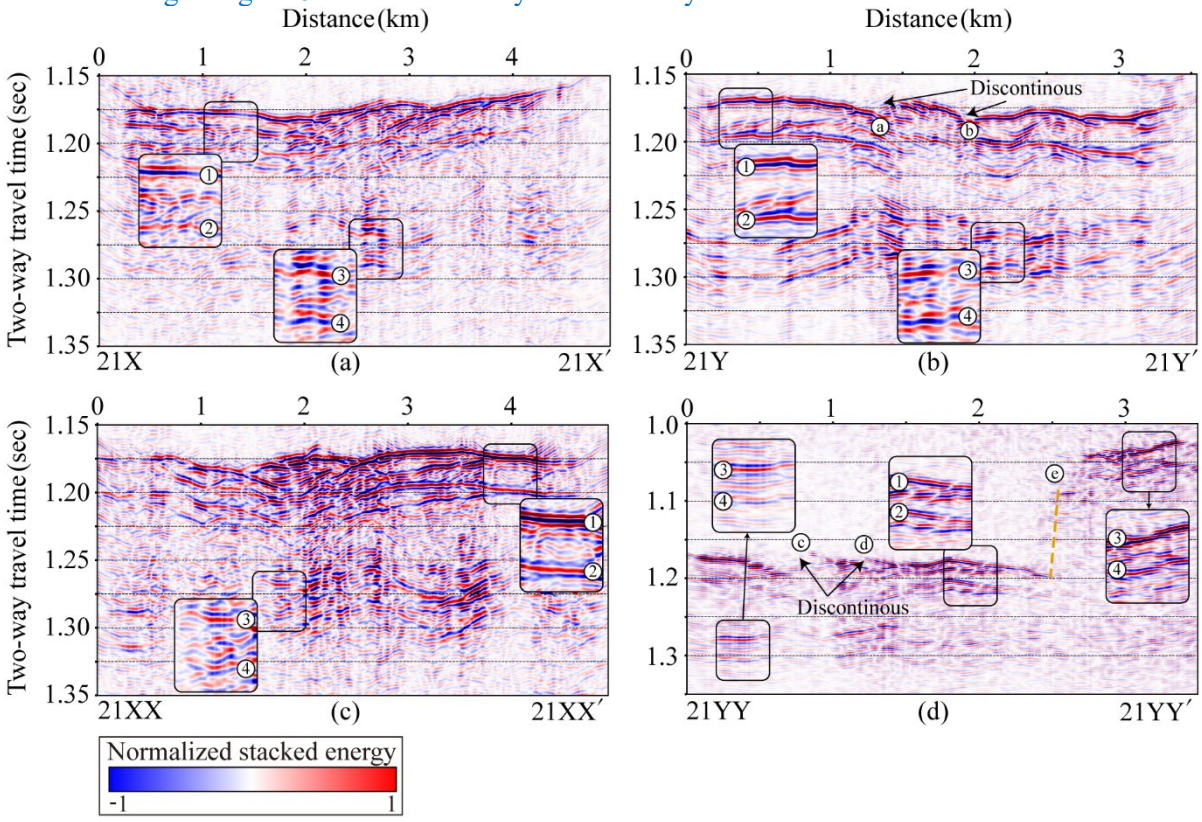

Figure 6: PSTM seismic sections for lines (a) 21X, (b) 21Y, (c) 21XX, and (d) 21YY prior to ghost removal. Ghost reflections appear 25–30 ms beneath the glacier–lake and lake–bed interfaces due to the 25 m source depth.

6. Scours: Really interesting interpretation, but I wonder how you can be sure these features are from depths rather than near surface or englacial crevassing? They look similar to observations from stations near shallow faults which show significant scattering or spurious arrivals from interactions with reflected phases. I also wonder if you could use cross correlation/autocorrelation with the direct

P to increase the coherence of the reflected arrivals and to better resolve the shape of these features? Further, while I see that the scour features interfere significantly in the synthetic, the observed amplitude is still comparable to the direct reflections, which is again not true in the data. I wonder if instead, the near surface scattering argument is invoked, would you expect significant defocusing and thus lower amplitude?

➔ We appreciate the reviewer's insightful comments. For clarity, the term "scour" was revised to "scour-like feature (SLF)" throughout the manuscript and figures.

The SLF structure is clearly observed along the Y-line but is not readily identifiable along the X-line. In particular, some end-shot records from the X-line exhibit overlapping signals between the ice–bedrock interface reflection and surface waves or crevasse-induced noise, which hinders interpretation. However, in the Y-line records, such scattering signals predominantly appear after TWT 1.5 seconds and are therefore clearly distinguishable from the depth range where the SLF structure is observed. Moreover, in the synthetic dataset, surface wave and crevasse-related noise do not overlap with the ice–bedrock interface reflection signals. Consequently, it is unlikely that the SLF signal could be misinterpreted as surface scattering or surface wave noise. Furthermore, the surface topography of the study area is very flat, and the shallow sediment layer exhibits a similar spatial distribution. Therefore, the likelihood of surface or shallow structures generating scattering signals that could be mistaken for SLF is very low. Additionally, no reflection patterns or polarity characteristics typical of SLF structures are observed in the shallow parts of the seismic profiles.

The synthetic velocity model is discretized, leading to diffraction signals around the SLF structure in the synthetic seismograms. These diffractions interfere with nearby reflectors during migration. As the reviewer noted, it is still possible to interpret these features as defocusing effects caused by near-surface scattering. However, given the geological and geophysical conditions of the site, we believe it is more likely that the SLF structure is located at the bottom of the glacier.

Nonetheless, to fully exclude the possibility of near-surface scattering or spurious arrivals from shallow fault zones, further verification is necessary. We agree with the reviewer that applying cross-correlation and autocorrelation techniques will strengthen the connection with direct P-waves and enable additional validation of reflection consistency. We are currently performing follow-up research using these methods, along with improved velocity modeling, to improve resolution and achieve greater accuracy in deep structural interpretation.

7. I am wondering about the firn velocity model used: If I do a linear interpolation, I see that the average firn velocity in the upper 25 meters is around 1800 m/s, consistent with what is stated in the text. However, a consistent feature of the firn is the steep velocity gradient/density near the surface which shallows with depth, which is very nonlinear. I believe this effect is probably small, but in terms of the raytracing, the incident angles of the incoming waves in the simulations of a linear vs nonlinear firn will be very different, which affects reflectivity. If you calculate your own Vs firn model, or if you use an empirical relation/calibration for your firn model, you could solve for a firn to ice transition depth which would be another interesting finding of the paper.

➔ We appreciate the reviewer's insightful comment regarding the firn velocity structure. As pointed out, firn velocity generally increases non-linearly with depth due to rapid density and velocity changes near the surface (Agnew et al., 2023; Picotti et al., 2024). However, accurately developing a site-specific firn velocity model remains very challenging in practice, since firn properties can vary greatly depending on factors like local compaction rates, the ratio of fresh to old snow, moisture content, and seasonal temperature changes.

In the study area above the D2 subglacial lake, field observations confirmed that the snow and firn surface is highly compacted. During fieldwork, the surface was so solid that it did not break under foot traffic. Additionally, when excavating about 5–10 cm to install receivers, we observed that the near-surface snow layer had a high density, similar to solid ice.

Quantitatively, the first-arrival travel times recorded by receivers directly above the shot points (offset = 0 m) ranged from approximately 10.6 to 15.5 ms. Considering the estimated shot depth of approximately 25 m, the apparent average velocity for the top 25 m is calculated to be approximately

1795 m/s (Figure R1).

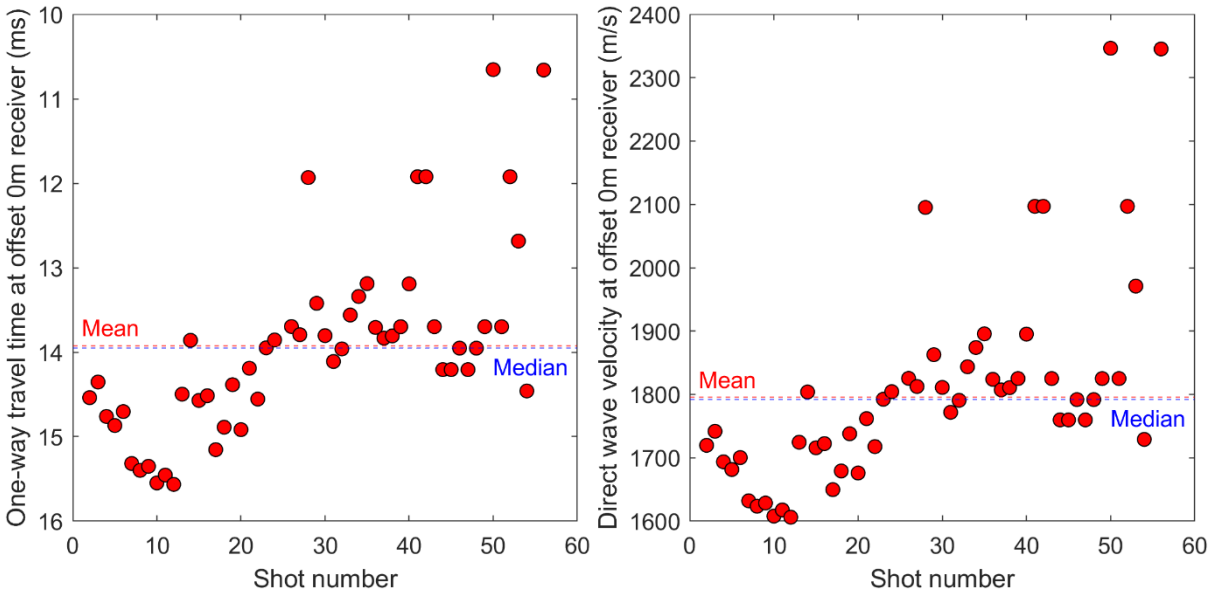

Figure R1: (Left) First-arrival travel times recorded at offset = 0 m along survey line 21X. (Right) Apparent velocity for the upper 0–25 m depth estimated based on the measured first-arrival times.

Additionally, the apparent velocity in the 0–25 m depth range, estimated from the ghost signal with an approximate delay of 28 ms, is about 1785 m/s. Velocity analysis of the shot records shows a three-layer structure: the direct wave velocity in the top layer (0–50 m depth) is roughly 1800 m/s; in the middle layer (50–100 m), the direct wave velocity increases to around 2600 m/s; and the refracted wave, related to glacial ice, has a velocity of approximately 3800 m/s (Figure R2). Accordingly, we revised Figure 4 to display the velocities of both direct and refracted wave, reflecting these considerations.

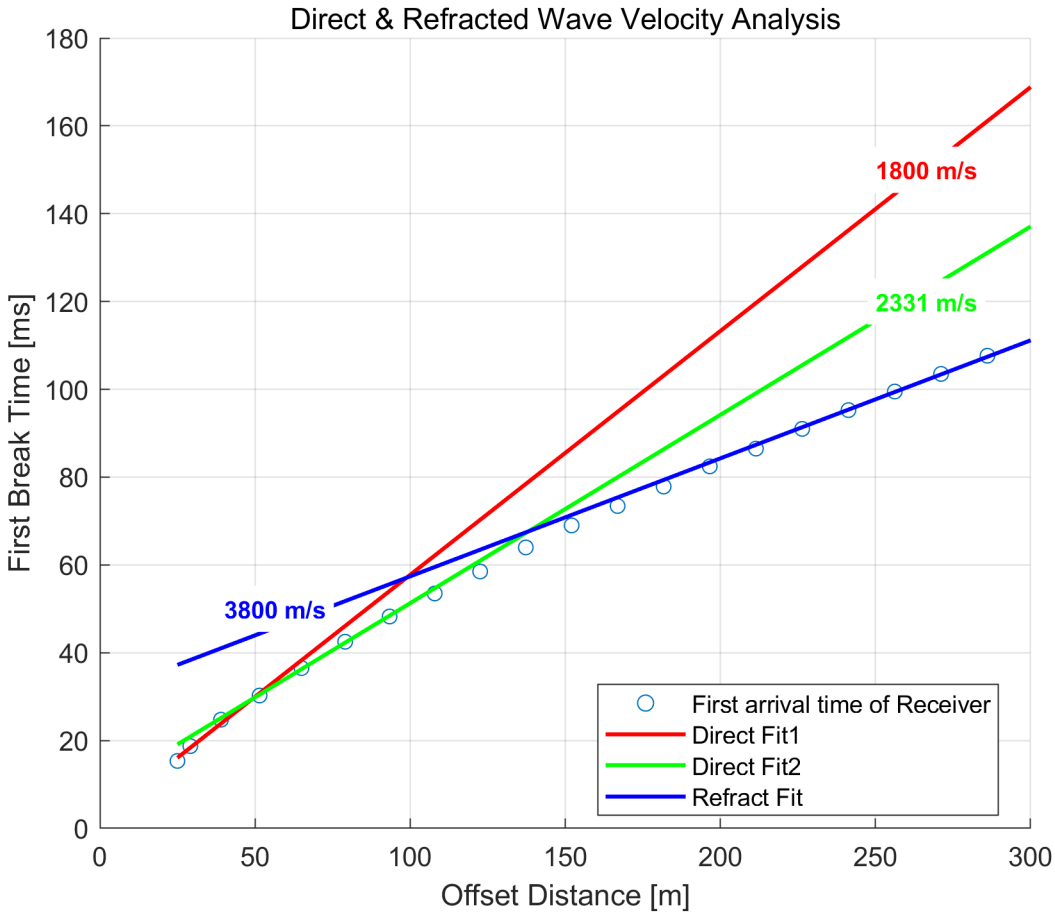

Figure R2: Direct and refracted wave velocities estimated from End-shot data (Shot record #9) along survey line 21X.

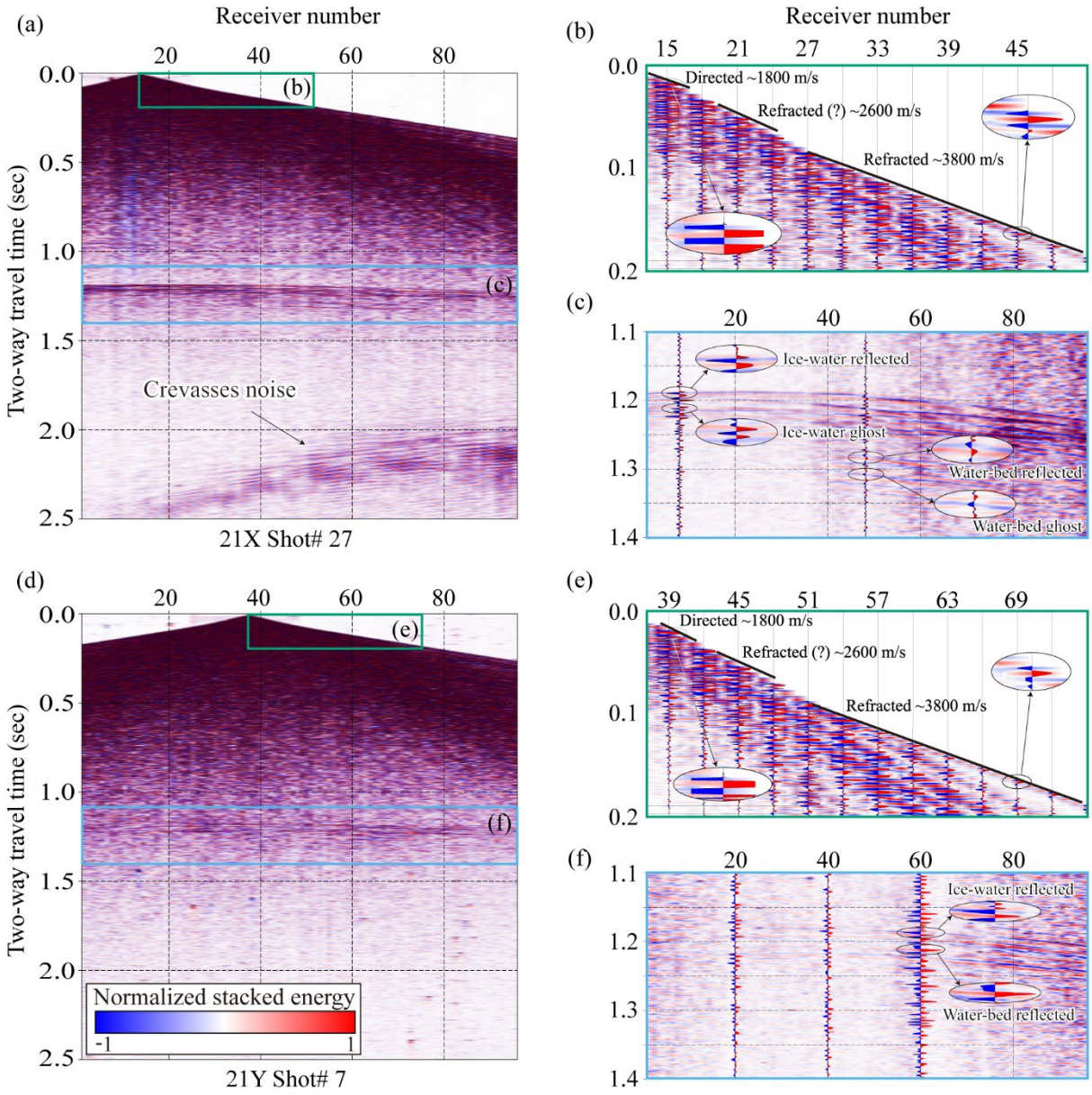

Figure 4: Raw shot records from seismic lines 21X (a) and 21Y (d). Panels (b) and (e) are zoomed-in views of the early arrival window (0.0–0.2 s) from panels (a) and (d), respectively, used to calculate the apparent velocities of the direct and refracted waves. These panels highlight that the first arrivals of both the direct wave (clipped for display) and the refracted wave exhibit positive polarity. The direct wave, propagating through the upper firn layer (0–25 m depth), shows an apparent velocity of approximately 1800 m/s, while the refracted wave traveling through glacier ice has an apparent velocity of about 3800 m/s. Panels (c) and (f) are zoomed-in views of the deeper arrivals (1.1–1.4 s) from panels (a) and (d), respectively. Reflections from the ice–water interface exhibit negative polarity, whereas those from the water–bed interface display positive polarity.

Based on the field observations, we applied a 1D velocity model assuming a linear increase in velocity from the surface down to 100 m depth, using an apparent velocity of approximately 1800 m/s for the upper 0–25 m layer. Although we attempted to apply nonlinear firn velocity models as suggested by the reviewer (e.g., Yang et al., 2024; Picotti, Carcione, & Pavan, 2024; Agnew et al., 2023), we found that, given the observed first-arrival times in this region, these models either yielded physically unrealistic results or led to numerical instabilities.

Nevertheless, we fully acknowledge the importance of more accurately representing the firn velocity structure. To this end, we are currently conducting additional data analysis and high-resolution velocity inversion, with the goal of applying more advanced firn velocity models such as those recently proposed by Agnew et al. (2023) and Picotti et al. (2024). These improvements will be incorporated into a future study to enhance the robustness and physical realism of the velocity model.

We have added content to the conclusion (Page 19, Line 371-374).

8. I wonder if the full processing scheme need be applied to the synthetic data. Given the extensive processing combined with the lack of ambient noise/crevasse scattering, the data should basically be clean enough to examine on its own. I understand for consistency's sake why the same processing is applied, but here, I would emphasize that the synthetics before and after processing remain pretty much the same. If they do not, that could point to artifacts being introduced in your processing scheme.

➔ As correctly pointed out, excessive or unnecessary processing steps may introduce artifacts, particularly in synthetic datasets that lack ambient noise and crevasse scattering. In response, we have revised our approach and now apply only the migration step to the synthetic data. We agree that this modification is more appropriate and better aligned with the purpose of using synthetic data. Accordingly, the main text has been updated to reflect this change. In addition, we have included both pre- and post-migration results of the synthetic dataset in the revised Supplementary Materials, allowing for transparent evaluation of any potential processing-related artifacts.
(Page 14, Line 274) We have revised from
"The same seismic processing sequence applied to the field data (Section 3.2, Fig. 5) was subsequently applied to the synthetic dataset to produce a PSTM image for comparison" to
"We applied just the migration step in the case of the synthetic dataset, as it is free of noise".

9. I think Figure 9a also has a polarity issue. This is showing the synthetic and observed seismic data shot gathers with arrivals corresponding to the glacier lake interface, but the first arrival in both synthetic and observed appear to be normal polarity as opposed to the reverse polarity that is stated. Am I interpreting these figures wrong? IN addition, back to the glacier-bed interface, the synthetic phases 3, 4 representing the glacier-bed and ghost have normal and reverse polarity respectively, while the field observations seem to have reverse and normal polarity respectively. Is this a color bar issue, or am I interpreting these images wrong?

➔ We apologize for the mistake in the previous version of Figure 9, where the polarity was displayed incorrectly during the figure's production. We have revised Figure 9 accordingly. In the updated figure, negative polarity in the wiggle traces is now correctly shown on the left (blue) and positive polarity on the right (red). Additionally, the figure has been enlarged for better visibility, and the previously incorrect time axis labeling has been corrected.

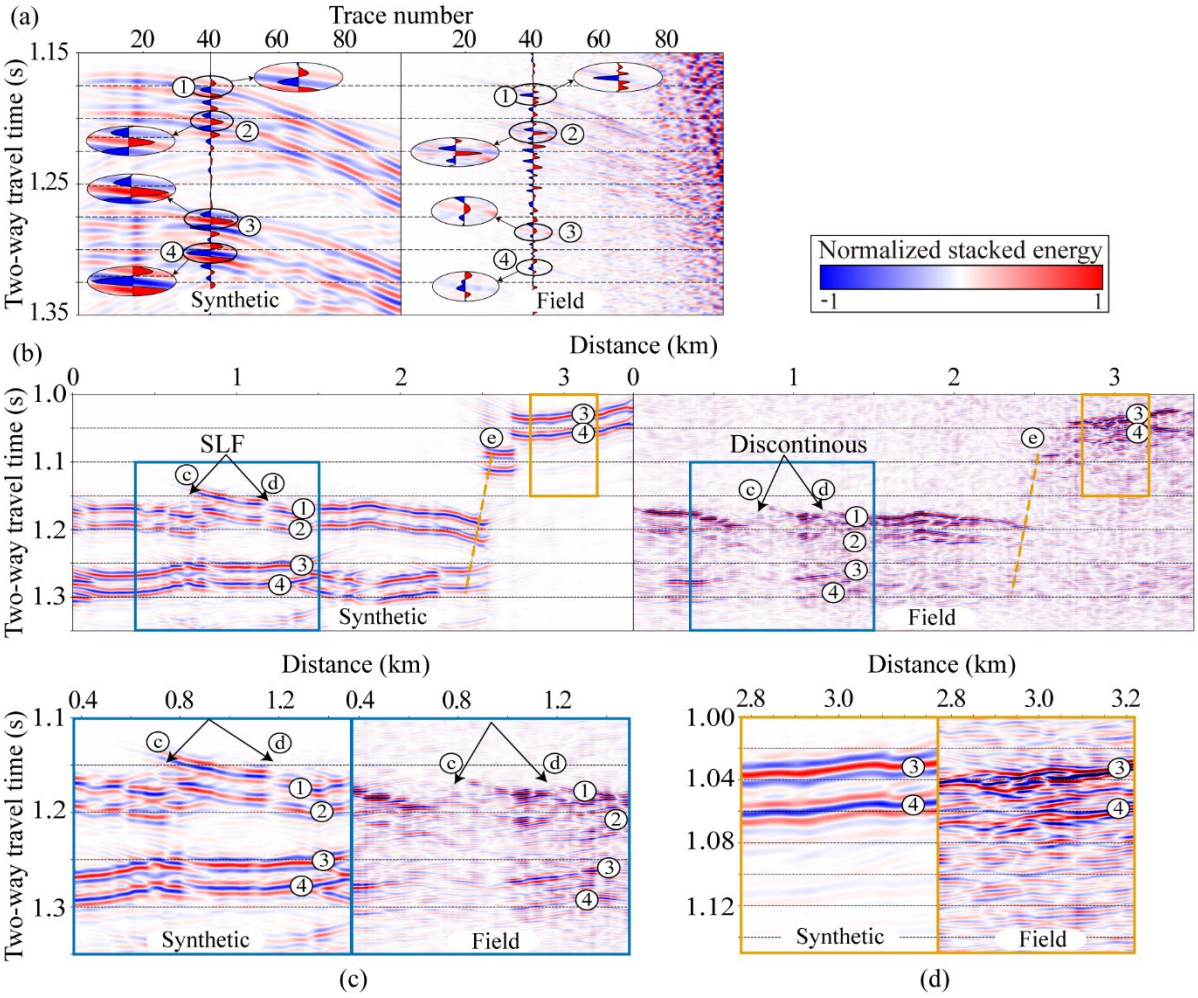

Figure 9: Comparison of synthetic and field seismic data. (a) Shot gather at the same location for synthetic (left) and 21YY field data (right). (b) PSTM comparison between the synthetic model and the 21YY line. (c) Enlarged views of discontinuous reflections (synthetic, field). (d) Comparison of dipping bed reflections (synthetic, field), showing shadow zones and steep basal topography.

10. On figure 9, again, the same issue with reflection coefficient used as the colorbar. Neither the migrated sections nor synthetics are showing reflection coefficient, but rather normalized amplitude.

➔ We have revised the colorbar label from "Reflection coefficient" to "Normalized stacked energy".

11. I think this gets into a slight issue I have with the results, which is that apart from travel time calculations, they are mainly qualitative. The velocity of the subsurface is assumed (water, bed) rather than estimated via something like AVO to give you actual reflectivity. This means that while yes, the synthetics have the same shape, their amplitudes are not consistent with each other both laterally and in time (later arrivals are significantly weaker). This is likely due to a combination of attenuation and structure, but it was unclear whether this is considered in the modeling. I do feel that this comparison is only relevant for the geometrical features such as the scour surfaces or the steep bed slopes.

➔ As described in our response to Comment 4, there are inherent physical limitations in conducting a reliable AVO analysis in this study. Due to the restricted offset range of the acquired data, we instead constructed a physically reasonable subsurface velocity model informed by previous literature and the

geological context of the study area. Based on this model, we generated synthetic seismograms. We fully acknowledge that the absolute amplitudes of the synthetic data may not perfectly match those of the field data. Therefore, rather than focusing on amplitude strength, the primary objective of our interpretation is to conduct qualitative structural analysis using the wave polarity and arrival times of key reflections, including reflected (PP) waves, ghost (pPP) waves, and lake-bottom reflected (PPPP) waves, as well as reflections from erosional surfaces and steep bedrock interfaces. Quantitative analysis is limited to depth estimation based on direct and refracted wave velocities.
The observed weakening of the ghost signal amplitudes is attributed to high attenuation within the firn layer near the surface, which cannot be explicitly modeled in our velocity structure due to its complex and variable physical properties. Consequently, some mismatch in amplitude is expected between the field and synthetic data.
Nevertheless, given the acquisition conditions, the qualitative match between synthetic and observed waveforms is enough to support the geometric interpretations in this study — specifically about ice thickness, lake depth, scour morphology, and steep basal boundaries. Therefore, our quantitative conclusions are limited to those parameters derived from geometry.

12. Additionally, why are the timings of the synthetics and field data off? The synthetics arrive consistently earlier than the observations. Does this mean the depth used is too shallow? Or the firn is not fully accounted for?

➔ The observed discrepancies arise in part from our use of a homogeneous synthetic model based on a representative velocity structure estimated from Shot Point 1, applied uniformly across the entire 21YY survey line. While the travel times at Shot Point 1 closely match the observed data, deviations may occur at other locations along the line, where travel times may appear faster or slightly misaligned.
These discrepancies are primarily attributed to uncertainties in the thickness and velocity of the firn and ice layers. As noted earlier, we are currently conducting additional data analysis and high-resolution velocity inversion to enable the application of an improved firn velocity model. This refinement will be incorporated in future work to enhance the accuracy of travel time predictions and waveform matching.

13. Generally, I am not exactly sure how the results compare to the previous estimates of the D2 boundaries. From my understanding, the seismic interpretation is that the lake is on the opposite side of the marked boundary in orange on Figure 3. This could be me confusing the direction of the cross sections, but I think that emphasis the need for more clarity about the geometry of the features described.

➔ Please refer to our response to the comment 2, where this issue is addressed in detail.

14. Figure 10: Could you provide a reference for the resolution of both the IPR and seismic data? Perhaps on the plot, add points for the individual datapoints for the IPR line, which looks sparser? Additionally, why is the seismic prediction almost always slightly thinner, on the order of tens of meters? I wonder if including the uncertainty bars would help show the agreement between the two.

➔ We appreciate the reviewer's comment. As the IPR (Ice-Penetrating Radar) survey line does not exactly coincide with the seismic survey line, it is not possible to present point-by-point comparisons of the raw data from both datasets. The IPR data used in this study is an interpolated 2D profile, and values were extracted specifically at the locations corresponding to the seismic survey line. Therefore, the spatial sampling intervals between the two datasets are consistent. It is also important to note that radar wave velocity in ice is extremely high ($V \approx 0.17$ m/ns), which results in a larger inherent uncertainty in depth estimation from the IPR data. To account for this, we have included the estimated uncertainty ranges for both the IPR and seismic data in the revised figures.

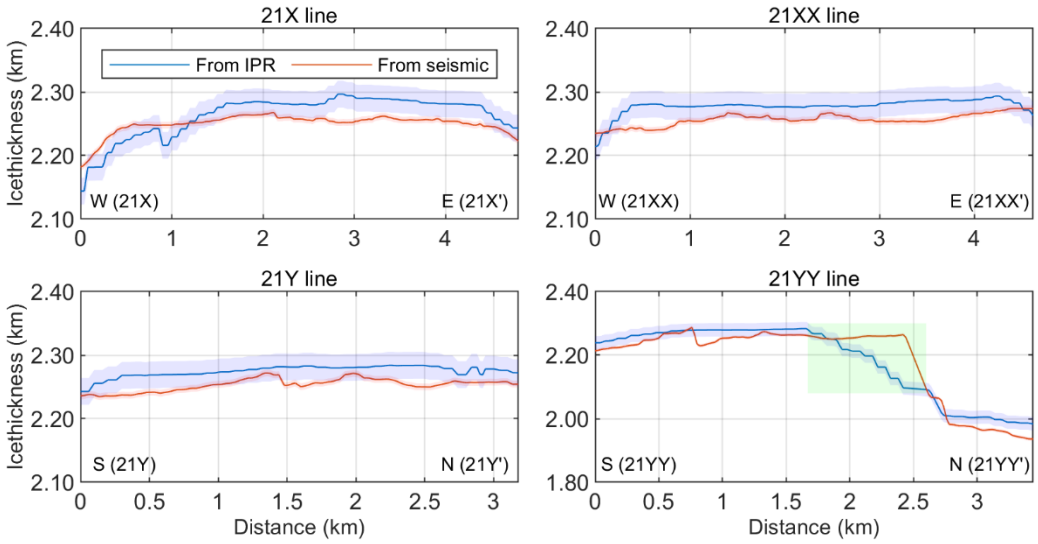

Figure 10

15. I think the use of published values for glacial firn, ice, water is fine for a starting model, but there is significant variation across estimates of these values (Yang et al. 2024; Picotti, Carcione, and Pavan 2024; Agnew et al. 2023). Also, these values or at least estimates of them should be visible during the velocity analysis stage. You could get a P wave velocity from the PP observation on the velocity/depth section and use that for the ice velocity in your model rather than a published one. Perhaps they will agree, but it's worth checking. Also, firn velocities for P wave can dip below 1 km/s (Yang et al. 2024), perhaps this can help explain the timing discrepancy you observe? Again, I wonder if you can get an estimate for the shallow velocity from the observed surface waves or pseudoacoustics.

➔ Please refer to our response to the comment 7, where this issue is addressed in detail.

My suggestions for revisions are as follows:

16. Data presentation and Interpretation: Provide a figure either in the main text or supplement that shows the clearest example of the reverse polarity reflection, perhaps accompanied by a synthetic. I think that part of the confusion is the difficulty in making out features on the record section as well as the slight inconsistencies in terminology. If you can also show the normal polarity reflection from the glacier-bed clearly, perhaps showing the actual waveform as done in 9a, the difference between the two regions would be immediately clear.

➔ Please refer to our response to the comment 9, where this issue is addressed in detail.

17. Modeling: Calculate Vp, Vs in firn and ice. It doesn't have to be in depth, as I understand that is not the point of the paper, but an average value or upper/lower bounds to at least confirm that your simple model is appropriate would help strengthen the interpretation and perhaps resolve some of the discrepancies between synthetics and observations. If you don't want to derive these values from the data, I suggest trying different basal models (wet sediment/till) to confirm that your simple 2d model matches the data best.

➔ Please refer to our response to Comment 7, where this issue is addressed in detail. The velocity model was constructed using P-wave (Vp) velocities derived from field data and supported by values reported

in previous studies. Due to limitations in the field data, it was not feasible to reliably extract S-wave (Vs) velocities; therefore, the synthetic model in this study was generated using Vp information only.

18. Supplementary information: Providing supplementary information, particularly on the data processing and interpretation, will clear up a lot of uncertainty about the signals that are observed. For example, the scour features; while you mention removal of surface waves and surface scattering, the detail given is not sufficient to explain exactly what the resultant signal we are seeing here is. Showing the raw data, or a panel with the data for each or important processing steps could help clarify your certainty in interpreting these features as structural rather than artifacts from the processing. I believe that at minimum a table which describes the processing parameters (anomalous amplitude attenuation, curvelet filtering, surface consistent amplitude compensation) is necessary for the sake of repeatability. Supplementary information can also contain a more thorough exploration of the model space.

➔ We have added additional results to the Supplementary Materials to show the outcomes at each stage of the data processing workflow. These additions help to further demonstrate that the observed scour structure is not an artifact caused by surface waves, surface scattering, or processing-induced effects, but rather represents a genuine subsurface structural signal. In addition, we have included the key processing parameters used at each step to enhance transparency and reproducibility.

Line Specific Comments within attached PDF.

➔ As the PDF file was missing and was not uploaded despite our request, we were unable to address the line comments. We have revised the manuscript and responded to the main comments raised above. If there are any important issues in the line comments that should be addressed in the manuscript, please notify us.

References:

Agnew, Ronan S., Roger A. Clark, Adam D. Booth, Alex M. Brisbourne, and Andrew M. Smith. 2023. "Measuring Seismic Attenuation in Polar Firn: Method and Application to Korff Ice Rise, West Antarctica." Journal of Glaciology 69 (278): 2075–86. https://doi.org/10.1017/jog.2023.82.

Horgan, Huw J., Laurine van Haastrecht, Richard B. Alley, Sridhar Anandakrishnan, Lucas H. Beem, Knut Christianson, Atsuhiro Muto, and Matthew R. Siegfried. 2021. "Grounding Zone Subglacial Properties from Calibrated Active-Source Seismic Methods." The Cryosphere 15 (4): 1863–80. https://doi.org/10.5194/tc-15-1863-2021.

Ju, H., Kang, S., Han, H., Beem, L. H., Ng, G., Chan, K., Kim, T., Lee, J., Lee, J., Kim, Y., and Pyun, S.: Airborne and Spaceborne Mapping and Analysis of the Subglacial Lake D2 in David Glacier, Terra Nova Bay, Antarctica, J. Geophys. Res.: Earth Surf., 130, https://doi.org/10.1029/2024jf008142, 2025.

Peters, L. E., S. Anandakrishnan, C. W. Holland, H. J. Horgan, D. D. Blankenship, and D. E. Voigt. 2008. "Seismic Detection of a Subglacial Lake near the South Pole, Antarctica." Geophysical Research Letters 35 (23). https://doi.org/10.1029/2008GL035704.

Picotti, Stefano, José M. Carcione, and Mauro Pavan. 2024. "Seismic Attenuation in Antarctic Firn." The Cryosphere 18 (1): 169–86. https://doi.org/10.5194/tc-18-169-2024.

Yang, Yan, Zhongwen Zhan, Martin Karrenbach, Auden Reid-McLaughlin, Ettore Biondi, Douglas A. Wiens, and Richard C. Aster. 2024. "Characterizing South Pole Firn Structure With Fiber Optic Sensing." Geophysical Research Letters 51 (13): e2024GL109183. https://doi.org/10.1029/2024GL109183.

Supplement of

Seismic data analysis for subglacial lake D2 beneath David Glacier, Antarctica

Hyeontae Ju, Seung-Goo Kang, et al.

Correspondence to: Seung-Goo Kang (ksg9322@kopri.re.kr)

S1. Seismic data processed parameters and results

This study utilized the Omega geophysical data processing platform (SLB) for seismic data processing. Among the various processing steps, we provide below the key parameters applied during procedures that directly influence the ice–bedrock interface signal, such as noise attenuation.

1. Anomalous amplitude attenuation (AAA) for the 1st round

AAA is a frequency-domain filtering technique designed to suppress spatially coherent anomalous amplitudes such as swell noise and rig noise, by comparing amplitude spectra across traces and attenuating outliers based on spatial median statistics. The method identifies frequency bands with anomalous energy by comparing each trace's amplitude spectrum within a spatial window to the median of its neighboring traces. Detected anomalies are either scaled or replaced using interpolated values from adjacent traces, preserving relative amplitude relationships. Key parameters include TIME, which defines the temporal window of threshold application; THRESHOLD FACTOR, which sets the amplitude level considered anomalous; and SPATIAL MEDIAN WIDTH, which specifies the number of adjacent traces used for median computation. Proper tuning of these parameters is essential to avoid signal distortion while effectively attenuating coherent noise. AAA is particularly useful in prestack data conditioning as it enhances seismic data quality without compromising true subsurface reflections (SLB, 2025a).

- SPATIAL MEDIAN WIDTH: 21 traces
- Threshold factor tables:

TIME	THRESHOLD FACTOR
0	15
1000	10
3000	7
4000	6

2. Curvelet transform-based filter for 1st round (Figure S43b)

Curvelet Transform is a multi-scale, multi-directional decomposition technique that provides a sparse representation of seismic data by capturing curved wavefronts more efficiently than conventional fourier or wavelet transforms. An important aspect of the Curvelet Transform implementation involves user-defined control over the scale and angle bounds that determine which components of the data will be transformed. The LOWER BOUND OF SCALE and HIGHER BOUND OF SCALE specify the range of spatial frequencies (scales) to be included in the transform. Lower scales correspond to coarse, low-frequency components, while higher scales capture fine, high-frequency structural details. The LOWER BOUND OF ANGLE and

HIGHER BOUND OF ANGLE define the directional sectors (angles) within each scale to be analyzed. This allows selective enhancement or suppression of events based on their dip or propagation direction (SLB, 2025b). Figure S1 illustrates how the f–k domain is partitioned into curvelet panels by scale and angle. Adjusting these bounds allows for targeted signal processing, such as isolating curved events or attenuating directionally coherent noise. These parameters provide valuable flexibility in customizing the transform for specific seismic applications.

- Panel manager

LOWER BOUND OF THE SCALE	HIGHER BOUND OF THE SCALE	LOWER BOUND OF THE ANGLE	HIGHER BOUND OF THE ANGLE
2	2	1	3
2	2	8	10
3	3	1	6
3	3	13	18
4	4	1	6
4	4	13	18

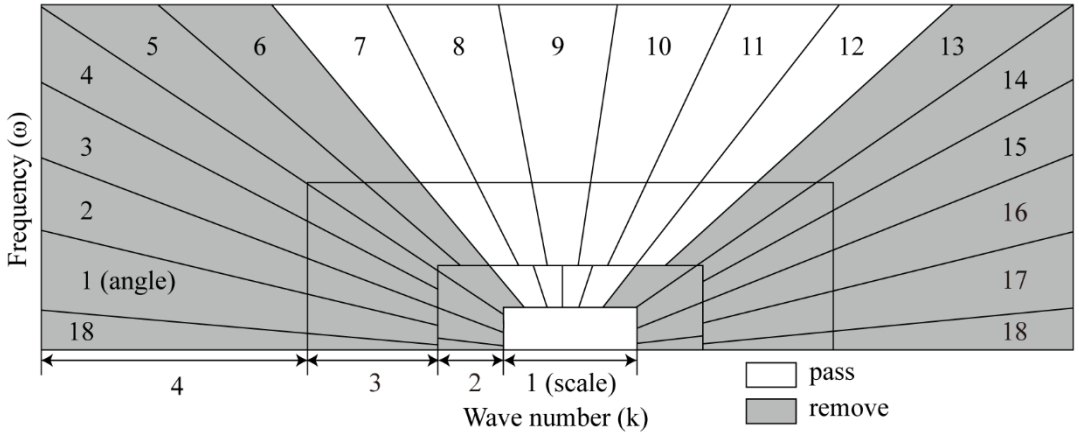

Figure S1: Illustration of the panel manager. In the f-k domain, the hatched area is identified as noise and removed accordingly.

3. Surface-consistent deconvolution

Surface-Consistent Deconvolution is a technique for generating and applying deconvolution operators that are consistent across seismic sources, receivers, offset ranges, and CMP locations (SLB, 2025c; Yilmaz, 2001).

Key processing parameters used in this workflow include:

- CONSTANT_ACOR_LENGTH = 100: Defines the half-length of the autocorrelation window used in operator design, balancing spectral resolution and filter stability.

- WHITE NOISE PERCENT = 0.01: Adds 1% white noise to stabilize the autocorrelation estimation and prevent over-whitening of the signal.
- PREDICTION DISTANCE = 2.5: Specifies the prediction lag in the predictive filter design; this parameter controls the temporal range of the filter's effect, influencing multiple suppression and resolution.

4. Anomalous amplitude attenuation (AAA) for the 2nd round
   - Spatial median width: 11 traces
   - Threshold factor tables:

Time	Threshold factor
0	8
1000	6
3000	4
4000	3

5. Curvelet transform-based filter for the 1st round: same as 1st round parameter

6. Frequency-offset coherent noise suppression (Figure S3.c)

The frequency–offset (F-X) Coherent Noise Suppression (FXCNS) module is designed to attenuate near-surface shot-generated coherent noise, such as dispersive surface waves and trapped modes, which interfere with primary seismic reflections, particularly in 3D shot or receiver gathers with irregular spatial sampling (Hildebrand, 1982). FXCNS operates in the frequency domain by modeling coherent noise using fan filters and estimating it in a least-squares sense for each trace based on local neighbors within a specified azimuthal sector. The estimated coherent noise is then subtracted from the original signal, preserving true reflection events (SLB, 2025d).

- LOW PASS VELOCITY: 100
- LOW STOP VELOCITY: 300
- HIGH PASS VELOCITY: 8000
- HIGH STOP VELOCITY: 10000

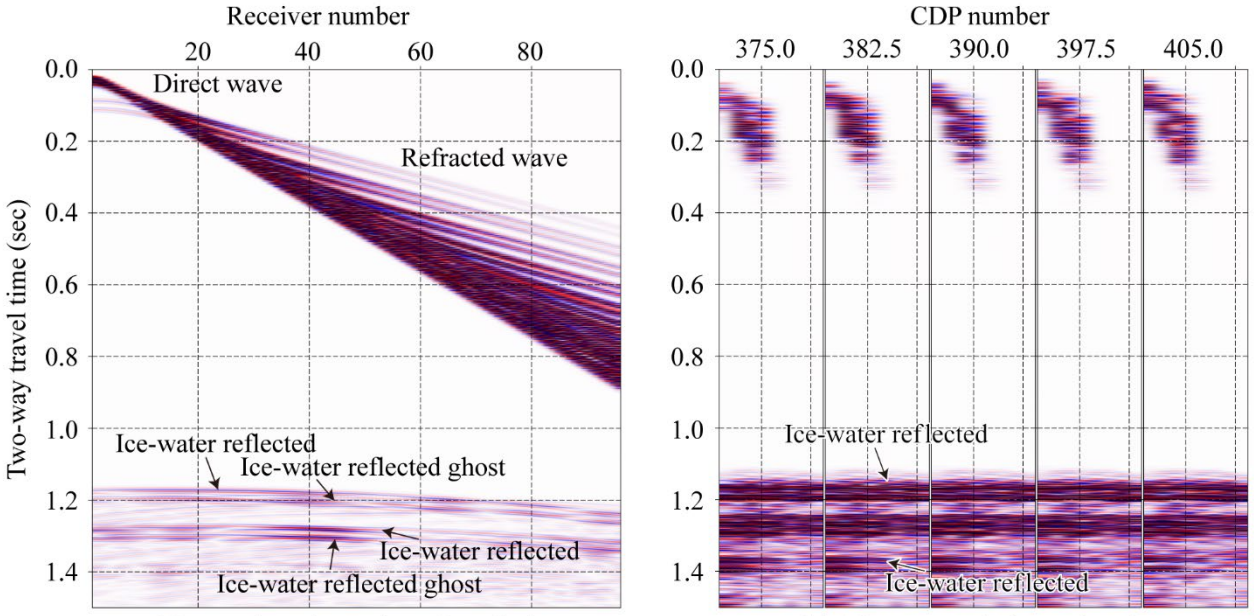

(a) Raw data shot gather of synthetic (b) After pre-stack time migration

Figure S2: Results before and after data processing. (a) Synthetic raw data of shot gather #1. (b) Result after pre-stack time migration.

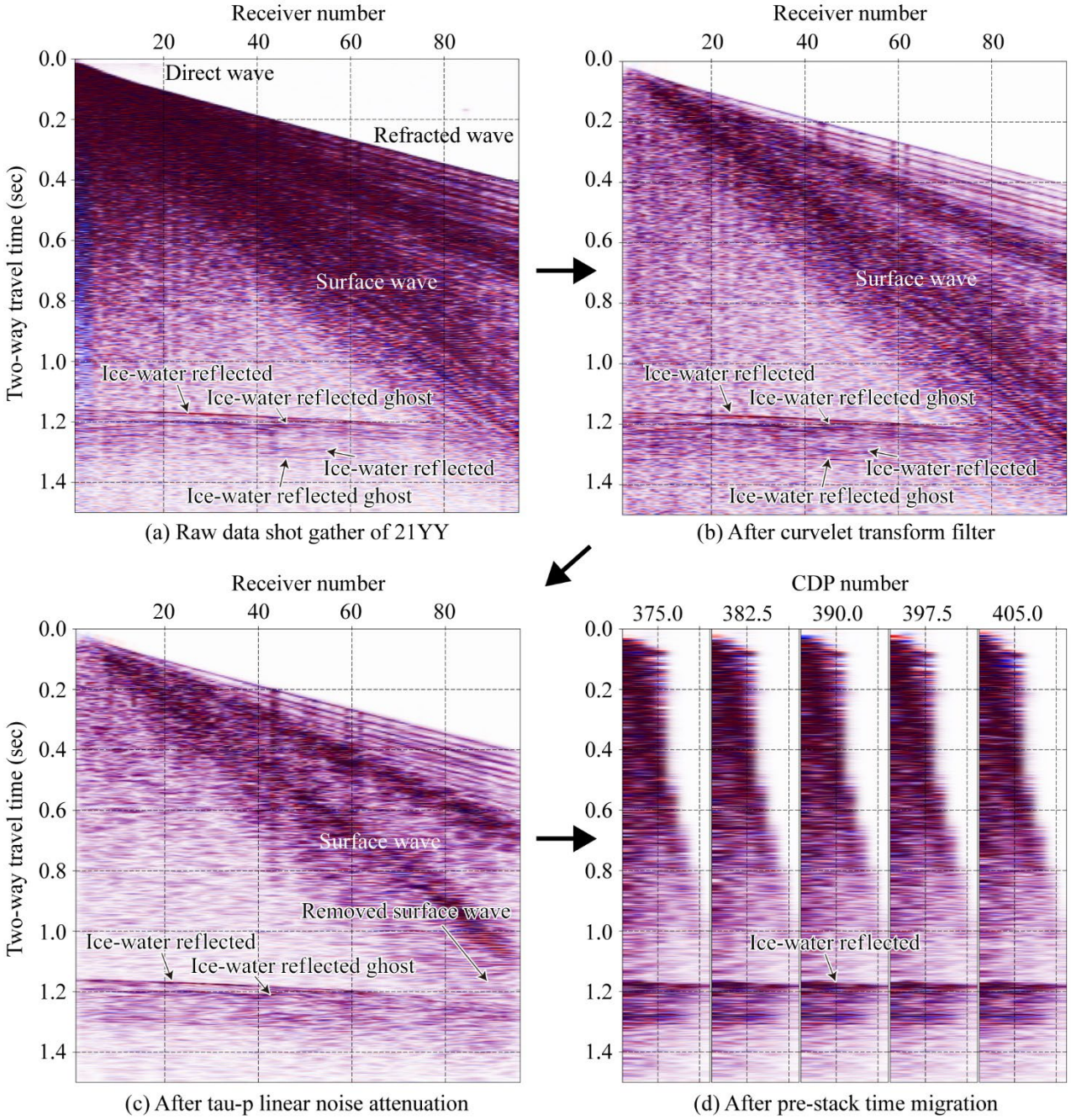

Figure S3: Results at each stage of data processing. (a) Shot gather #1 from 21YY. (b) Removal of high-frequency random noise and coherent linear noise. (c) Application of a frequency-offset coherent noise filter and tau-p linear noise attenuation for surface wave removal. (d) Result after applying pre-stack time migration.

References

Hildebrand, S. T.: Two representations of the fan filter, Geophysics, 47, 957–959, https://doi.org/10.1190/1.1441363, 1982.

SLB: *Omega Geophysical Processing System – Anomalous Amplitude Noise Attenuation (ANOMALOUS_AMP_ATTEN) Module Documentation*, Version 27.14, SLB manual, Houston, TX, 2025a.

SLB: *Omega Geophysical Processing System – Curvelet Transform (CURVELET_TRANSFORM) Module Documentation*, Version 22.1, SLB manual, Houston, TX, 2025b.

SLB: *Omega Geophysical Processing System – Surface-Consistent Deconvolution Analysis (SC_DCN_SPCTRL_ANL) Module Documentation*, Version 13.18, SLB manual, Houston, TX, 2025c.

SLB: *Omega Geophysical Processing System – F-X Coherent Noise Suppression (FXCNS) Module Documentation*, Version 3.16, SLB manual, Houston, TX, 2025d.

Yilmaz, Ö.: Seismic data analysis: Processing, Inversion, and Interpretation of Seismic Data, Appendix B.8 (Surface-Consistent Deconvolution), Society of Exploration Geophysicists, 262–266 pp., 2001.